

UNIVERSITY OF ILLINOIS

..... 19.....

THIS IS TO CERTIFY THAT THE THESIS PREPARED UNDER MY SUPERVISION BY

.....

ENTITLED.....

.....

IS APPROVED BY ME AS FULFILLING THIS PART OF THE REQUIREMENTS FOR THE

DEGREE OF.....

.....

.....

Instructor in Charge

APPROVED:

Charles F. Zuker

Richard C. Alkire

HEAD OF DEPARTMENT OF..... Chemical Engineering

Viscoelastic Properties of Polystyrene Lattices

by
Felix Lee Song

**Thesis for the Degree of
Bachelor of Science in Chemical Engineering**

**College of Liberal Arts and Sciences
The University of Illinois
at
Urbana-Champaign**

May 1988

Abstract

The objective of this study was to examine the rheological behavior of different sized polystyrene lattices and see whether current theoretical models can be used to accurately describe their behavior. Attempts were also made to obtain data for mixed particle lattices, however only measurements for homogeneous particles were taken due to flocculation problems. Comparison of experimental data as a function of volume fraction for particles with diameters of 103.9, 382, and 503.9nm indicate that no one model could accurately describe all three systems. Divergence of data from theory occurred at high volume fractions with all three systems.

Table of Contents

Abstract	i
Table of Contents	ii
Table of Figures	iii
1.0 Acknowledgements	1
2.0 Survey of Literature	2-10
2.1 Relationship Between Shear Modulus and Inter-particle Forces	2-6
2.2 Calculation of Diffuse Layer Potential	6-8
2.3 Packing Arrangements	8
2.4 Previous Work	8
2.5 Theoretical Shear Modulus Models	9-10
3.0 Experimental Methods	11-21
3.1 Materials	11
3.2 Formation of Polystyrene Particles by Emulsion Polymerization	11-14
3.3 Procedure for Cleaning the Emulsions	14-15
3.4 Concentration of Polystyrene Emulsions	15-17
3.5 Measurement of Shear Modulus	17-20
3.6 Operation of Modeling Programs for Shear Modulus	20
4.0 Results and Discussion	21-39
4.1 Experimental Observations and Data	21-27
4.2 Results of Modeling Studies	28-39
5.0 Conclusion	40
6.0 Recommendations	41
Bibliography	42-43
Appendix	44-47
Nomenclature	48-49

Table of Figures and Tables

Figure 3a:	Emulsion Synthesis Apparatus	12
Table 1:	Emulsion Polymerization Reagents	13
Figure 3b:	Schematic of Pressurizing Tank	16
Figure 3c:	Block diagram of Shearometer Device	18
Figure 3d:	Shearometer Wave Propagation Cell	19
Figure 4-1a	TEM Photograph of 103.9nm particles	23
Figure 4-1b	TEM Photograph of 382nm particles	24
Figure 4-1c	TEM Photograph of 523.4nm particles	25
Table 2:	Shear Modulus Measurements (103.9nm in 10^{-3} & 10^{-4}M NaCl)	26
Table 3:	Shear Modulus Measurements (382 & 523.4nm in 10^{-4}M NaCl)	27
Table 4:	Values of Surface Potential in RLSAP & RLSALCP Model	29
Table 5:	Values of Surface Potential in RLSACP & RLSAPDHS Model	30
Figure 4-2a	Graph of Shear Modulus vs. Volume Fraction	31
Figure 4-2bi	Shear Mod. vs. Vol. Fraction of 103.9nm in 10^{-3} M NaCl with Models Assuming FCC Packing	32
Figure 4-2bii	Shear Mod. vs. Vol. Fraction of 103.9nm in 10^{-3} M NaCl with Models Assuming RCP Packing	33
Figure 4-2ci	Shear Mod. vs. Vol. Fraction of 103.9nm in 10^{-4} M NaCl with Models Assuming FCC Packing	34
Figure 4-2cii	Shear Mod. vs. Vol. Fraction of 103.9nm in 10^{-4} M NaCl with Models Assuming RCP Packing	35
Figure 4-2di	Shear Mod. vs. Vol. Fraction of 382nm in 10^{-4} M NaCl with Models Assuming FCC Packing	36
Figure 4-2dii	Shear Mod. vs. Vol. Fraction of 382nm in 10^{-4} M NaCl with Models Assuming RCP Packing	37
Figure 4-2ei	Shear Mod. vs. Vol. Fraction of 523.4nm in 10^{-4} M NaCl with Models Assuming FCC Packing	38
Figure 4-2eii	Shear Mod. vs. Vol. Fraction of 523.4nm in 10^{-4} M NaCl with Models Assuming RCP Packing	39
Figure A1	Shear Wave Propagation Cell	47

1.0 Acknowledgements

I would would first of all like to thank Professor Zukoski for the opportunity of working for him and learning what graduate school would be like. I also thank him for the concern he had for my research and my future.

I would also like to thank my thesis advisor, Jeanne Chang, for her help with my thesis, her patience for the problems I had as well as the discussions about innumerable things.

Dan Klingenberg and Greg Bogush for their help with the computer and concerns for my graduate studies

Louise Marshall, Liang Bin Chen, and Jeanne Chang for TEM pictures taken

Lastly the Chemical Engineering Department for the educational experience.

2.0 Survey of Literature

2.1 Relationship between Shear Modulus and Inter-particle Forces

Polymer lattices have become extremely useful in the study of colloidal phenomena. The advantage of using polymer lattices, particularly polystyrene, is that there are established methods to synthesize homogenous, spherical particles. The spherical geometry of these particles is especially attractive because it allows rheological data from this system to be compared to several theoretical models which have been developed to explain the particle-particle interaction that occur in solution.

In dilute colloidal suspensions, particles can move freely and are only subject to Brownian motion. As the concentration of particles increases, the repulsive forces of adjacent particles become significant. These repulsive forces limit the range of motion a particle can travel. The particles then begin to form an ordered lattice in order to minimize the free energy of the system. This orderly array can cause iridescence to occur for homogeneous systems containing particles of a certain size range. In addition to the formation of a lattice, as the suspension becomes increasingly more concentrated, the suspension begins to behave less as a Newtonian and as a more viscoelastic fluid. Therefore highly concentrated colloidal systems can be useful in determining the relationships between the bulk rheological properties of the system and the inter-particle forces. Inter-particle forces such as electrolyte concentration, particle size, and the diffuse double-layer potential of the particles and their relationship to bulk rheological properties of colloidal suspensions can be examined.

The rheological property that was measured for these experiments was the shear modulus as a function of volume fraction. The shear modulus can be related to inter-particle forces by a model that assumes pair-pair interactions.

In trying to describe the shear modulus as a function of the double-layer interaction potential, Buscall [1] uses a force balance to describe the interactions between nearest neighbor particles. Using the simplified case of two particle

N = Avogadro's number
 I = Ionic strength (mol/liter)

The Van der Waals potential energy, V_A , between two identical particles in a concentrated suspension can be expressed as [5] :

$$V_A = -A [12 \pi]^{-1} \left[(x^2 + 2x)^{-1} + (2x+1)^{-1} + 2 \ln \frac{x^2 + 2x}{x^2 + 2x + 1} \right] \quad (4)$$

where:

A = Hamaker constant

$$x = \frac{R-2a}{2a}$$

In a concentrated colloidal system, inter-particle interactions cannot be assumed to be occurring only in pairs, instead a particle interacts with several particles. The sum of these interactions can be taken as the sum of interactions between pairs of particles and therefore the potential energy of one particle interacting with several can be expressed as:

$$PE = (1/2) \sum (V_T) \quad (5)$$

where n = # of nearest neighbors

The interaction potential of a system is calculated by determining the particle-particle interactions between pairs and then average over all the pairs by assuming some sort of structure. In this experiment we have assumed a solid state structure exists within the suspension.

R is defined as the center to center distance of two particles. R_{eq} is defined as [6-8] :

$$R_{eq} = \frac{2a \phi_m}{\phi} \quad (6)$$

where:

ϕ = volume fraction of particles to suspension
 a = particle radius
 ϕ_m = a constant which describes the volume fraction of hcp and fcc packing (.74) or bcc packing (.64)

The shear modulus of a concentrated lattice can be related to the interaction potential energy between particles by an electrostatic-geometrical analysis [1] as:

$$G_0 = \frac{\alpha \delta^2 V}{R \delta R^2} \quad (7)$$

$$\text{with } \alpha = (3/32) \phi_m n$$

$$n = \# \text{ nearest neighbors}$$

There are three assumptions for this relationship between shear modulus and interaction potential. This derivation assumes that a small shear strain is applied so that the frequency of the applied strain is small compared to the relaxation time of the strained lattice. Secondly, the relaxation time of the electrical double-layer is also small compared to the relaxation time of the strained lattice. Finally, it is assumed that a solid state structure is formed within the suspension.

Assuming that in the equation $V_T = V_A + V_R$ that the Van der Waals forces are negligible at particle distance R , the total potential simplifies to $V_T = V_R$.

Differentiating equation (2) twice with respect to R and then substituting into equation (7) gives an equation for shear modulus as a function of interaction potential as:

$$G_0 = \frac{4\pi\alpha \epsilon\epsilon_0 (\psi_0)^2}{R^4} (\kappa^2 R^2 + 2\kappa R + 2 \exp(-\kappa(R-2a))) \quad (8)$$

From this equation it can be seen that the shear modulus is an exponential function that depends on ionic strength (κ : eqn.3); and volume fraction (R : eqn. 6).

Therefore by measuring the shear modulus and knowing the ionic strength and volume fraction, it is possible to determine the surface potential, particle size, or maximum packing fraction.

Russel [9] also uses solid state theories in order to relate shear modulus to interaction potential and derives a similar equation:

$$G_0 = \frac{(1/2)n \rho (R_{eq})^2 \delta^2 V_T R_{eq}}{\delta R^2} \quad (9)$$

$$\text{where } \rho = \text{number particles}/m^3$$

In deriving this equation, Russel uses an energy balance in finding this

relationship while Buscall uses a force balance. Note that in both cases, Russel's and Buscall's equations are similar and differ only in a constant. This is due to differing simplifying assumptions. Whereas Buscall attempted to estimate all the relative spatial components and integrated, Russel neglected all the directional component except for one.

2.2 Calculation of Diffuse Layer Potential, Ψ_0

Both the Buscall equation (eqn.7) and Russel (eqn.9) have an equation for shear modulus dependent on Ψ_0 which is the diffuse layer potential, also called the surface potential. A rigorous calculation for this parameter can be done by solving the nonlinear Poisson- Boltzman (PB) equation. However, this is a difficult equation to solve and simpler approximations for this equation have been developed, two of which are the Linear Superposition Approximation (LSA) and the Derjaguin Approximation. The two approximations only consider the case of large separation and small separation between two particles, respectively. The determination of whether adjacent particles are considered to be close or far apart is defined by the dimensionless parameter $\alpha\kappa$, which is the product of the particle radius and the inverse double-layer thickness of a particle. If $\alpha\kappa$ is small, it means that the separation between particles is large and the interaction potential can be calculated by LSA. The Linear Superposition Approximation assumes that the overall potential between two particles is simply the sum of the individual particle potentials in the absence of its neighbor or:

$$\Psi(R) = \Psi(r_1) + \Psi(r_2) \quad (10)$$

R is the distance from the center of one particle to the center of the second particle and r_1 r_2 are the radii of the respective particles. The interaction potential is derived by examining the change in free energy as the two spherical particles are brought together from an infinite distant apart to R . This leads to equation (2) shown previously.

$$V_R = 4\pi(1/R)\epsilon_0\epsilon a^2 \psi_0^2 \exp[-\kappa(R-2a)] \quad (2)$$

a = particle radius (m)

ϵ = relative permittivity

ϵ_0 = permittivity of free space

R = distance from center to center of adjacent particles

ψ_0 = diffuse layer potential with condition $\psi_d < 50$ mV

For small separations between particles, or large κa is. The electrostatic interaction potential can be approximated by the Derjaguin Approximation (DA). The DA assumes that the particles are so close together that the region between them can be described as an interaction between two parallel plates. The equation to describe this potential is:

$$V_R = 2\pi\epsilon\epsilon_0 a \psi_0^2 \ln(1 + \exp(-\kappa(R-2a))) \quad (11)$$

It has been assumed for both the LSA and DA that κ is independent of volume fraction within the suspension. However, since the particles themselves are charged, the concentration of ions within the suspension may not necessarily be the same as the surrounding dialysate, due to the semi-permeable membrane which separates them. It is possible that the concentration of ions within the membrane may be higher than that in the dialysate since ions will diffuse into the suspension to balance the charge on the particle. This is called Donnan equilibrium and it implies that the ionic strength in the suspension may be actually higher than in the dialysate. Thus κ would depend on ionic strength of the electrolytes and of the particle surface charge. The effect of Donnan equilibrium has been taken into account in other models dealing with interaction potentials, notably by the models of Penfold and Ramsey [10] and Voeglti [11]. Penfold and Ramsey accounts for the Donnan equilibrium by assuming that there is a linear relationship between ionic strength and volume fraction, while Voeglti assumes that the ionic strength increases as a function of $\cosh(z\Psi)$ where z is the valence number of the electrolyte and

8

$$\Psi = 3 \phi \sigma / 21ac(1-\phi) 10^3 N.$$

Ψ = phase potential (dimensionless)

N = Avogadro's number

σ = surface charge (C/m^2)

2.3 Packing Arrangements

As mentioned earlier, it has been assumed that solid state theories could be used to model concentrated colloidal suspensions. The assumption that the suspension may only take bcc or fcc arrangements is not completely valid since the system is a liquid and the particles have the possibility of moving about and forming random close packing arrangements. The benefits of assuming fcc or bcc is that the coordination number, n , and the maximum volume fraction, ϕ_m , is defined. With random close packing arrangements these parameters are ill defined and therefore make calculations for interaction potentials difficult.

2.4 Previous Work

Lindsay and Chaikin [12-14] and Buscall [1] have studied the elasticity of polystyrene suspensions. Lindsay and Chaikin have worked with particle diameters of 109nm and 220nm, but their work is in the region of low volume fractions, <0.10 . Buscall has worked in volume fractions up to 0.40 but with particle diameters of less than 200nm. Buscall has modeled his results with the force-balance derived shear modulus equation (8) and assumed an fcc arrangement within the suspension. Neither researchers have worked in the regime of volume fractions higher than 0.40 or of particle sizes greater than 200nm.

2.5 Theoretical Shear Modulus Models

There were four programs used to model the shear modulus as a function of volume fraction. The for programs used were RLSAP, RLSACP, RLSALCP, and RLSAPDHS. These programs were developed by Jeanne Chang. [21] In all of these programs, the shear modulus equation by Russel was used (eqn.9)

$$G_0 = (1/2)n \rho (R_{eq})^2 \frac{\delta^2 V_T R_{eq}}{\delta R^2} \quad (9)$$

using the LSA approximation for V_T (eqn. 2)

$$V_R = 4\pi(1/R) \epsilon_0 \epsilon a^2 \psi_0^2 \exp[-\kappa(R-2a)] \quad (2)$$

where κ is:

$$\kappa = \frac{2e^2 N 10^{-3} I}{\epsilon_0 \epsilon kT} \quad (3)$$

The packing arrangements considered for the suspensions was either FCC or BCC. Body centered close packing was not considered, since it does not model very well the shear behavior of suspensions with a high volume fraction.

RLSAP used the Russel equation for shear modulus and calculated the surface potential in terms of ψ_0 . RLSACP and RLSALCP tried to consider the effect of the Donnan equilibrium where:

$$I = [\text{electrolyte in dialysate}] + [\text{counterions for the particle}]$$

With the RLSACP model, the Penfold and Ramsey assumption was used to account for the counterion effect. Since the Penfold and Ramsey model assumed that ionic strength was a linear function of volume fraction, κ also became a function of volume fraction, and the concentration of the surrounding dialysate was assumed the same as the initial ionic concentration of the dialysate. RLSALCP, which was a model developed by Voeglti [11], assumed that although the concentration of counterions was the same as assumed by Penfold and Ramsey, the concentration of the electrolyte within the suspension would be slightly less than the electrolyte concentration outside the dialysis membrane due to charge balances. This assumption would cause the

value of Voegli's ionic concentration to be slightly less than Penfold and Ramsey's ionic concentration. In effect, RLSALCP would give a shear modulus curve that would rise less steeply as RLSACP.

The RLSAPDHS model comes from Russel and his coworkers study of freezing phenomena. They observed that a suspension undergoes a change from a randomly oriented mixture to a highly ordered one as the volume fraction increased. This ordered state occurred at a volume fraction of 45-55%. However this volume fraction was based on an effective hard sphere diameter. The hard sphere radius is greater than the radius of the actual radius of a particle. Russel made the assumption that this phase transition occurred at a V/kT on the order of one. The RLSAPDHS model also made two other assumptions. The first assumption was that the surface charge of a particle at its hard sphere radius was the same as its surface. The other assumption was that the particles may never touch each other. The RLSAPDHS program used the assumption that V/kT is equal to one to find the hard sphere radius and from this radius, an effective maximum packing fraction.

3.0 Experimental Methods

3.1 Materials

Styrene monomer used in all particle synthesis was supplied by Aldrich Chemical Inc. (Milwaukee Wis.) with a purity of 99%. Before use, the monomer was distilled at 34^o C and 30 psia to remove inhibitors. Solvent used for all reactions and dialysis was water purified by a Barnstead NANOpure II, which provided water with an electrical resistance >18 megaohm/cm. Other chemicals used for particle synthesis were:

Potassium Hydroxide, ACS grade [Mallinckrodt, Paris, Kentucky, Lot KMHY]

Potassium Persulfate, Analytical grade [Mallinckrodt, Lot KVEH]

Potassium Phosphate monobasic, ACS grade [Mallinckrodt, Lot KTCS]

Sodium Chloride, ACS grade [EK Industries Inc, Addison, Ill, Lot 015042]

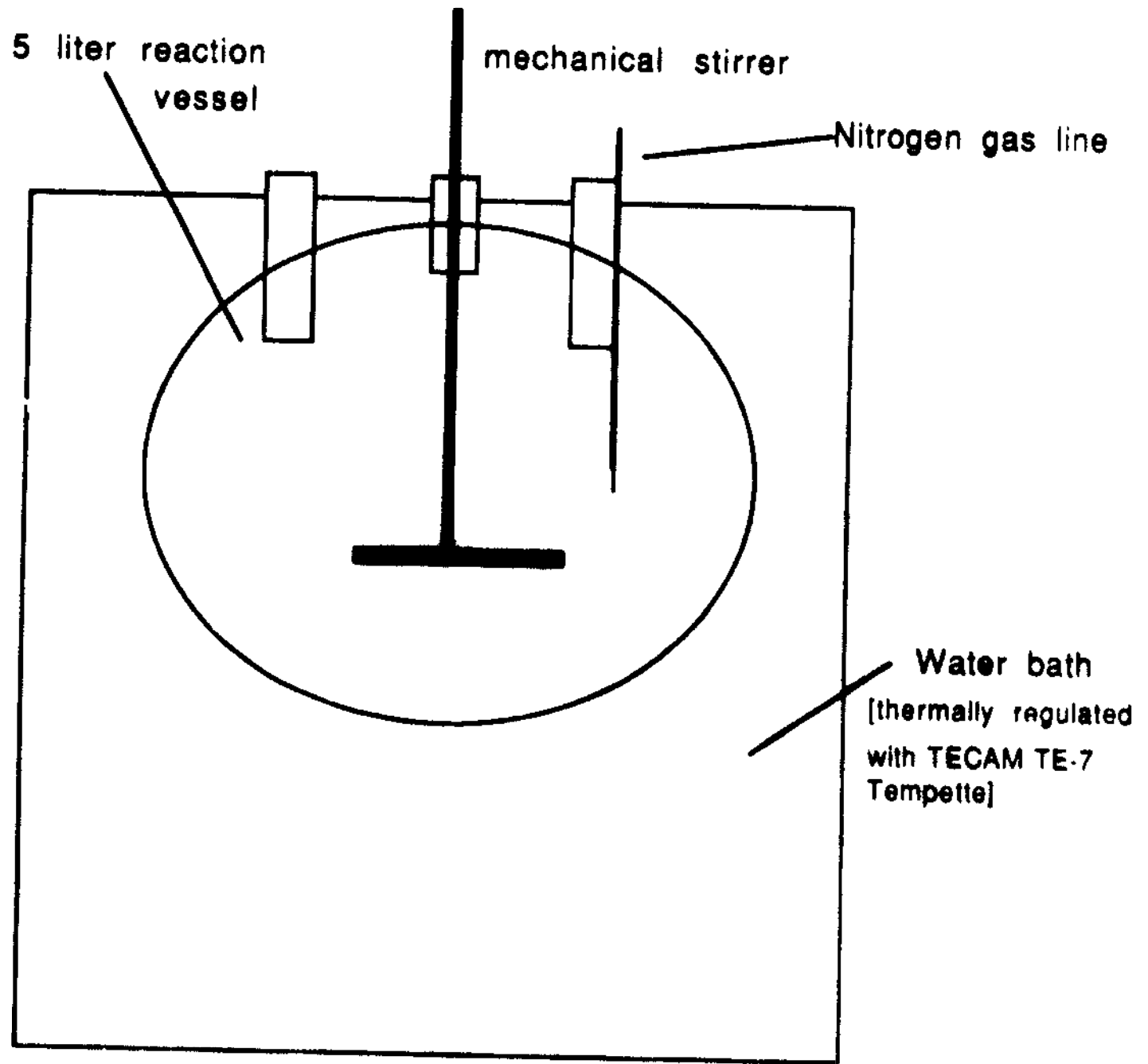
Styrene Sulfonic Acid-Sodium Salt, ACS grade [Polysciences Inc, Warrington PA
Lot 35681]

3.2 Formation of Polystyrene Particles by Emulsifier-Free Emulsion Polymerization

Two methods were used to produce particles, depending on the size of particle synthesized.

The method described by Juang and Krieger [15] was used to synthesize 523.9nm and 386.2nm in diameter particles. A 5 liter 3-necked flask, with a mechanical stirrer through the center neck and the other necks sealed with ground glass stoppers was used as the reaction vessel. The reactor temperature was held constant in a water bath with a Tecam TE-7 Tempette. While the reactants were added to the reaction vessel, stirrer speed

Figure 3a: Emulsion Synthesis Apparatus



Reagents	103.9nm	386.2nm	523.9nm	
DI water	3554ml	3364ml	3600ml	
NaCl	6.4824g	8.5700g	0.6312g	
KOH	1.1947g	0.8960g		0
KH ₂ PO ₄	0.0363g	0.0272g		0
NaSS	5.0058g	0.9991g	0 g	
Styrene	446ml	634.6 ml	403 ml	

was kept at 150-160 rpm. Figure 3a is a schematic of the reaction set-up. Table 1 lists, in order of addition, the amount of reactants used for each emulsion polymerization. Distilled water, less 30ml, was first added to the reactor and the temperature allowed to reach steady-state. The solid reagents were dissolved in withheld 30 ml of water before addition to the reactor. When the water within the reactor reached steady-state, NaCl, KOH, and KH_2O_4 were dissolved in 25 ml of water and added to the reactor. After 20 minutes, the distilled styrene monomer was added and the reactor temperature was allowed to reach steady state. After the reactor reached steady-state, a nitrogen purge line was attached to the reactor to purge the reactor and its contents of oxygen. After 15 minutes of purging, the initiator, $\text{K}_2\text{S}_2\text{O}_8$ was dissolved in 10 ml of water and added to the reactor. After 5 minutes of mixing, the stirrer speed was decreased to 70-75rpm to prevent foaming. When the reactor contents become an opaque white color, the purge line was removed, the reactor was stoppered, and the system was stirred for 24 hours.

The method used for the synthesis of the 103.9nm particles was from Liu and Krieger (16). The procedure was exactly the same except for the addition of an ionic comonomer, sodium styrene sulfonate. The comonomer was added to the reactor along with the addition of NaCl, KOH, and KH_2PO_4 .

After 24 hours of mixing, the reactor was disassembled and the emulsion poured through a funnel lined with glass wool into a Nalgene container. A sample was removed and placed on a copper grid for a TEM (Transmission Electron Microscope) picture to be taken of the particles. Homogeneity of the particles and measurements of average particle size were checked.

3.3 Procedure for Cleaning the Emulsions

The newly synthesized emulsions were cleaned to remove unreacted monomer and unwanted electrolyte. This was done by dialysis. The dialysate was an aqueous solution of 10^{-4}M NaCl.

The emulsion was poured into 50cm-long dialysis sacks. The dialysis sacks were knotted at the bottom and the top was secured with a clip. The filled dialysis sacks were then placed in a 25 liter container filled with 10^{-4}M NaCl solution. Prior to use, the

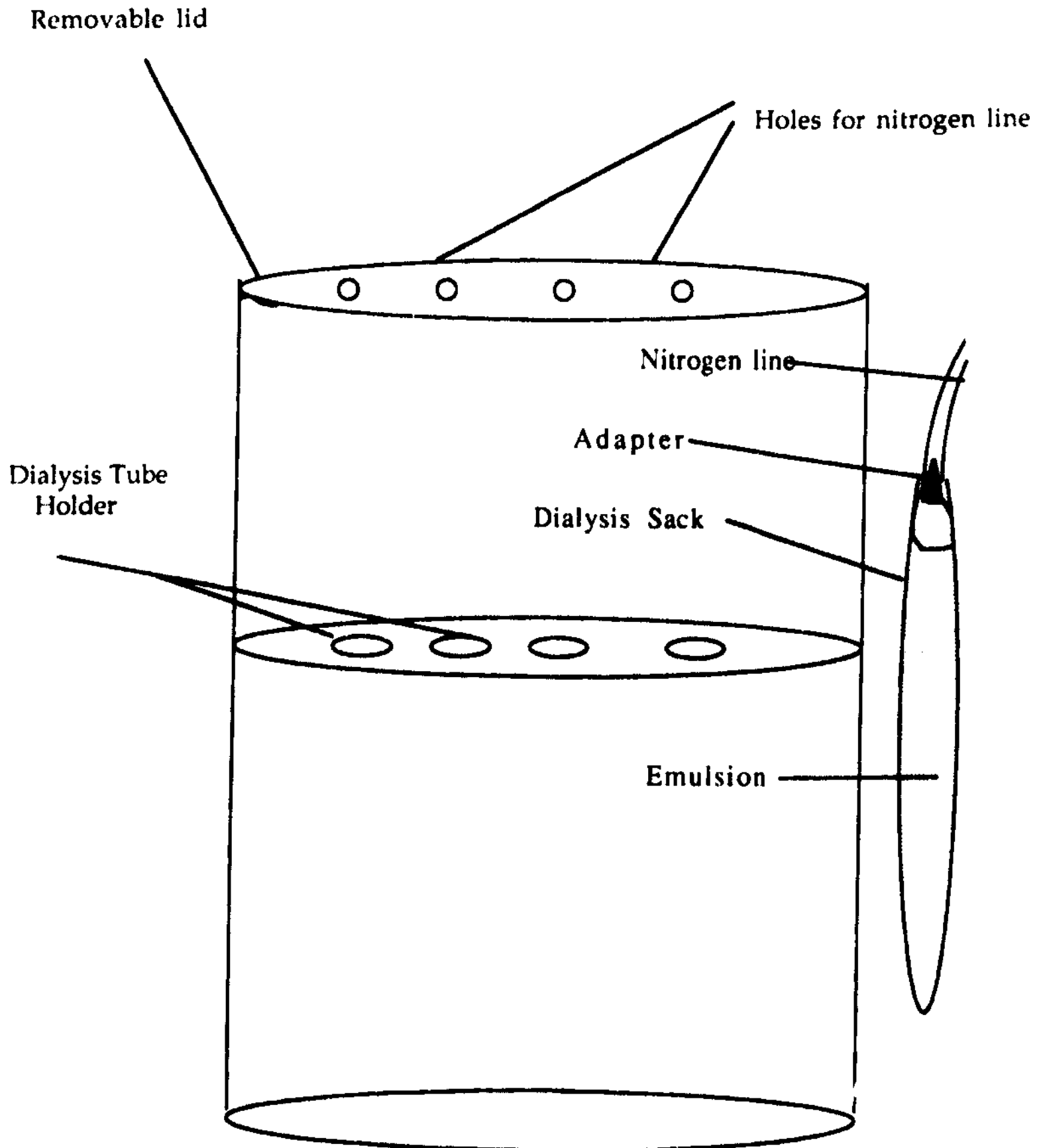
dialysate's conductivity had been measured with a conductivity meter (Altex Conductivity Bridge, Model RC-20 by Beckman) . Typical conductivity readings for fresh dialysate was 13.9 micro-Siemens. Once a day, the dialysate was removed and its conductivity measured. Fresh dialysate was then made, its conductivity measured, and then used. Dialysis of the particles was determined to be completed when no change in conductivity was observed in a twenty-four hour period. The contents of the dialysis sacks were then emptied into a container and stored for concentration.

3.4 Concentration of Polystyrene Emulsions

Concentration of polystyrene emulsions was done by using pressure to force the liquid within the emulsion past a dialysis membrane. Concentration of the emulsion was necessary to prepare the emulsion for shear modulus measurements.

Emulsion to be pressurized was held in 50cm long dialysis sacks which were attached to nitrogen gas lines to force liquid out of the emulsion. The dialysis sacks were held in a container filled with a 10^{-4} M NaCl while pressurizing, to prevent the dialysis membrane from drying out and to maintain the electrolyte concentration within the emulsion. Before being filled with the emulsion, the dialysis sacks were double-knotted at the bottom and submerged in a graduated cylinder filled with dialysate solution. The dialysis sack was then attached to a nitrogen line and inflated to 1 psig to check for leaks in the membrane. If no leaks were observed, the sack was filled with emulsion and the top fitted with an adapter to allow a nitrogen line to be attached to the dialysis sack. The adapter was a 1" long 0.5" diameter tube fitted to a reducer that would fit a 3/16" tube. The top of the dialysis sack was fitted over the .5" tube and secured by hose clamps. After the dialysis sack was fitted with the adapter, the assembly was resubmerged in a graduated cylinder filled with dialysate and gas pressure applied to check for leaks. If no leaks were found, the assembly was placed in a container that held several dialysis sacks as they were being concentrated. This container had a rack inside to keep the dialysis sacks vertical as they were being concentrated (Fig 3b). The container was filled with dialysate to maintain electrolyte concentration within the emulsion and to prevent the dialysis membrane from drying out.

The pressure used in concentrating the emulsion was 1 psig. Pressurizing continued

Figure 3c : Schematic of Pressurizing Tank

Note: The container shown above only has capacity for four dialysis sacks actual containers had a capacity for 10 sacks.

until the emulsion was 1/6 of its original volume. The sacks were then removed. For the larger particles, 523.9nm and 382nm, iridescence was observed. The concentrated emulsions were then checked for flocculates. If flocculates were found, they were manually broken up and redissolved into solution. An emulsion that was ready for shearing would have the consistency of a thick gel. Emulsions that had not reached this state were placed under pressure and concentrated further. Samples ready to be sheared were clipped snugly and stored in jars filled with 10^{-4} molar dialysate solution.

3.5 Measurement of Shear Modulus

The shear modulus of the polystyrene lattices was done by using a Rank Pulse Shearometer by Pen Kem Inc. An explanation of how the device works and a derivation of the equation to calculate shear modulus from the wave propagation velocity is contained in Appendix A1.

To measure the shear modulus of a suspension, the shearometer must be zeroed. This is done by selecting the option "Set Up Mode" from the computer directory and decreasing the separation between the two plates until a waveform appears. The separation between the two plates was changed by using the height adjustment screw. After receiving the waveform, the plates were separated apart by a quarter turn of the adjustment screw and the position locked by a restraining collar. The upper transducer was then removed and the suspension placed into the cell and the upper transducer replaced. The shearometer was then placed into "V-Sep mode" and the density setting at 1000 kg/m^3 . Measurements of the suspension were taken from 0.5mm to 5.25mm of plate separation. The shear modulus was displayed on the computer screen. (see Fig 3c & 3d)

After finding the initial shear modulus, the procedure was repeated a second time from 5.25mm to 0.5mm in 0.25mm increments. If the second readings were within 10% of the initial readings, no additional readings were taken. If the difference between the two readings was greater than 10%, another set of measurements was taken by starting at 0.5mm and 5.25 mm and working inward in 0.25mm increments. The highest and lowest shear modulus measurements were discarded. The shear modulus recorded was for a suspension that was 1000 kg/m^3 , we need to find the actual density of the suspension to find the true modulus. After determining the shear modulus of the suspension, a sample

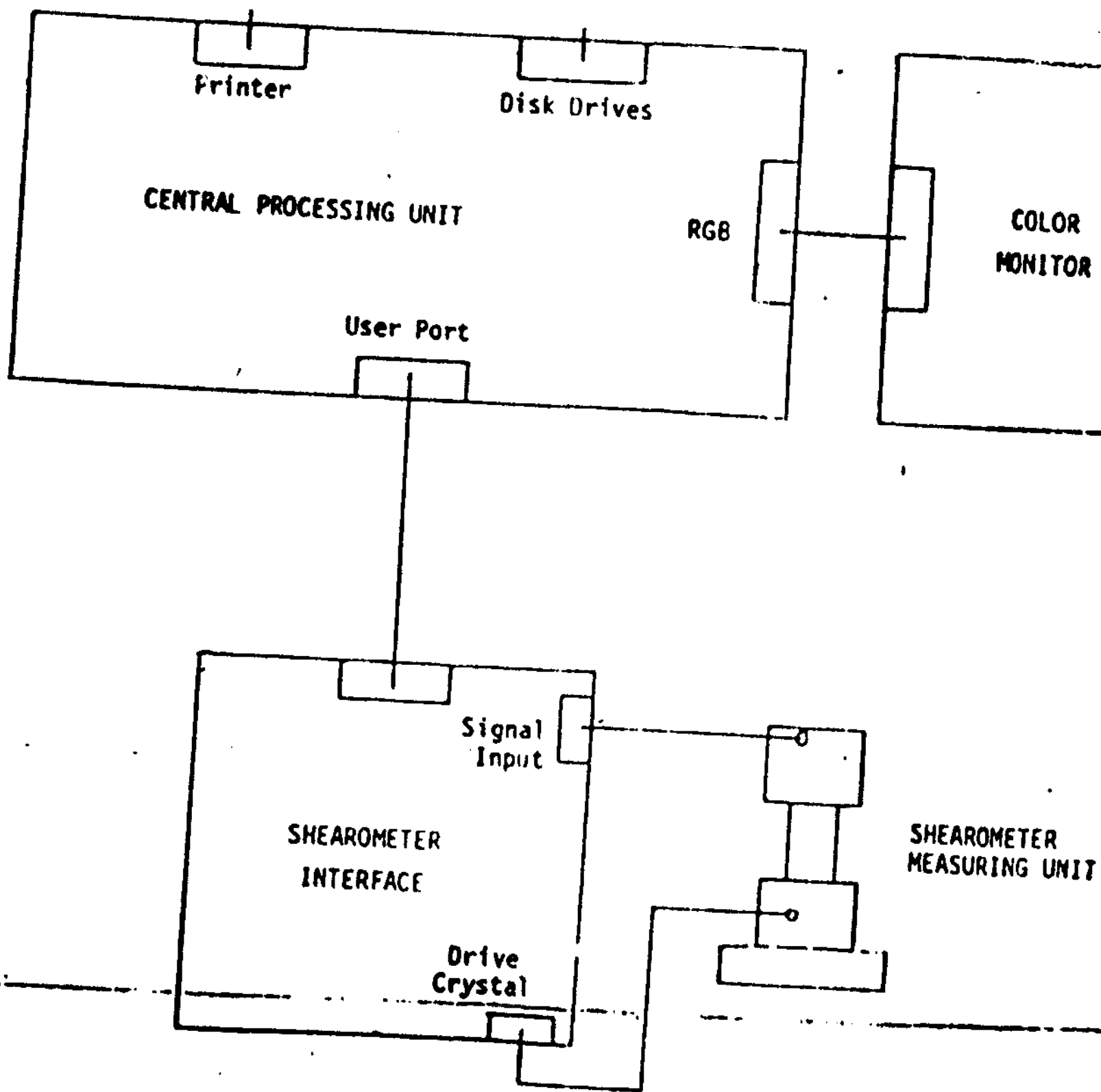


Figure 10: Block diagram of computer system

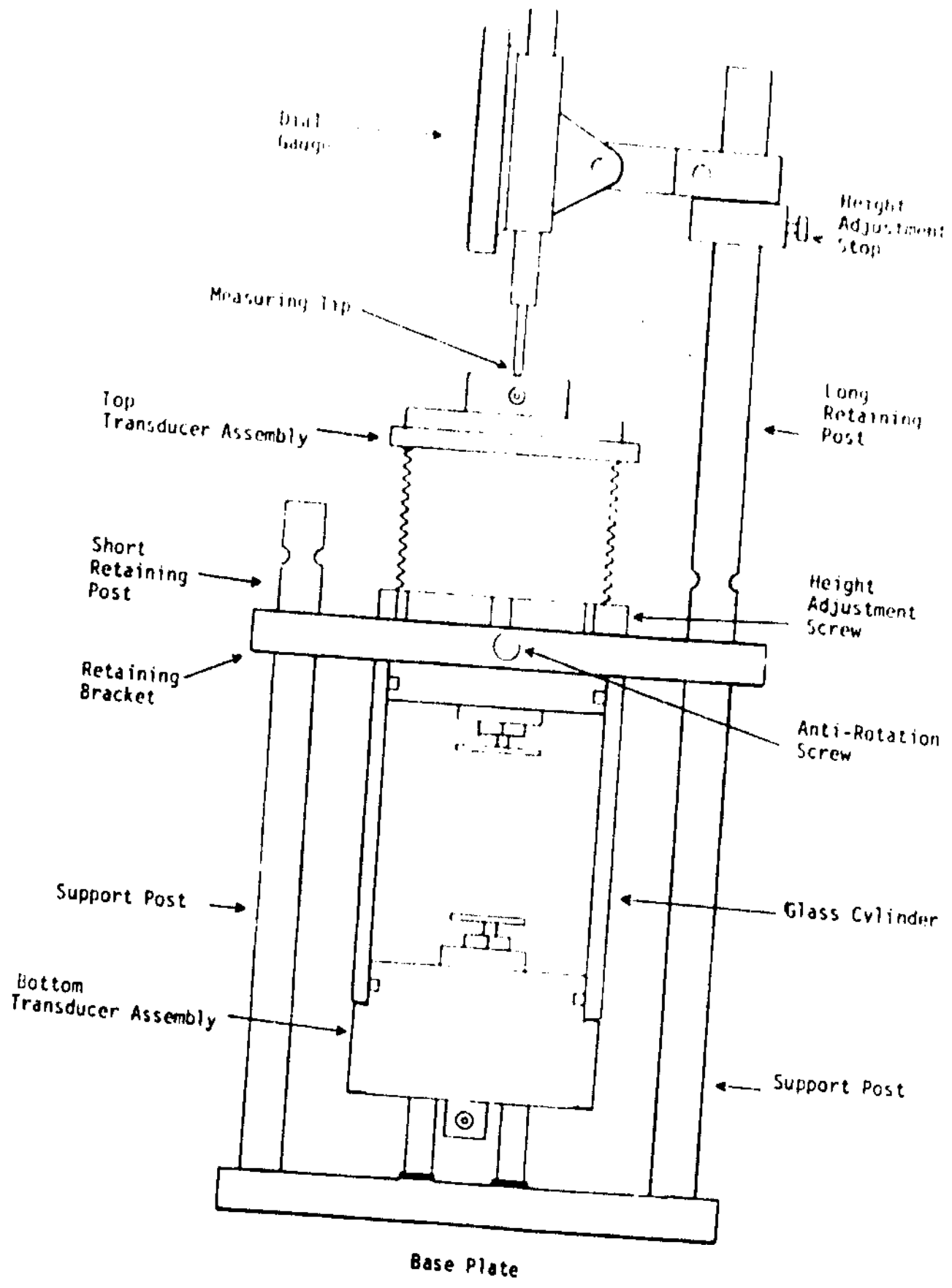


Figure 2d. Temperature Law Construction (2 of 2)

of the suspension was removed and placed in a dry, clean sample bottle to be dried in a 100° C oven. The weight of the bottle, weight of bottle and suspension, and the weight of the bottle and residue was recorded. By knowing the shear modulus at a density of 1000, and the mass fraction of the suspension; the actual shear and volume fraction of the suspension can be calculated by using these equations:

$$G_{ACT.} = G_{1000} \frac{\rho_{act}}{1000 \text{ kg/cm}^3}$$

G_{ACT} = shear mod. at actual density

ρ_{act} = actual density (kg/m³)

G_{1000} = shear modulus (Pa)

Volume Fraction=

$$\frac{\text{mass residue} \times (1.055 \text{ g/cm}^3 \text{ polystyrene})}{[\text{mass soln.} - \text{mass residue}] (1 \text{ ml/1g water}) + (\text{mass residue})(1 \text{ ml/1.055 g polystyrene})}$$

The suspension remaining in the shearometer was placed back into the dialysis sack. The sack was clipped snugly or loosely depending on whether a lower or higher volume fraction was desired for the next shear modulus measurement. The dialysis sacks were then allowed to sit in 10⁻⁴M NaCl for two days to allow the suspension to come to equilibrium with its surrounding before another set of measurements were taken.

3.6 Operation of Modeling Programs for Shear Modulus

The modeling programs used were, RLSACP, RLSAP, RLSALCP, RLSAPDHS. Two possible solid state structures were modeled, FCC ($\phi_m = .74$) and RCP ($\phi_m = .64$). The program used a least squares fit of the data in order to obtain a value for ψ . The surface potential the only adjustable parameter, and acceptable values were between 10-150mV.

4.0 Results and Discussion

4.1 Experimental Data and Observations

The original focus of my thesis work was to examine the shear modulus of polystyrene latices in 10^{-3}M NaCl. But due to flocculation problems the electrolyte concentration was reduced to 10^{-4} NaCl. However some of the problems that occurred were interesting and worth mentioning.

The particles synthesized by the method described by Juang and Krieger [15] seems to be less tolerant for the quicker methods of emulsion cleaning. This observation was made when attempts were made at cleaning the particles by centrifugation. The quick method was to centrifuge the emulsion and exchange the supernatant with distilled water and resuspend the particles. This process was done again two more times, once with distilled water and then with dialysate. Previously synthesized 503.3nm particles had been synthesized and cleaned by this method, leading to irreversible flocculation. It did not matter whether the speed of centrifugation was high and time short or if the centrifugation speed was slow and time long. Times and speeds were varied from 1000rpm for 5 hours to 15,000rpm for 15 minutes. The centrifugation time was determined by how long it took the supernatant to become free of particles. However, the 103.9nm particles, synthesized with an ionic comonomer [17] could withstand centrifugation for 15 hours at 15,000rpm. Although the particle size was five times as small and so the interparticle distance required for flocculation was also smaller, it seems that the difference in size could explain the great difference the two particles had toward centrifugation.

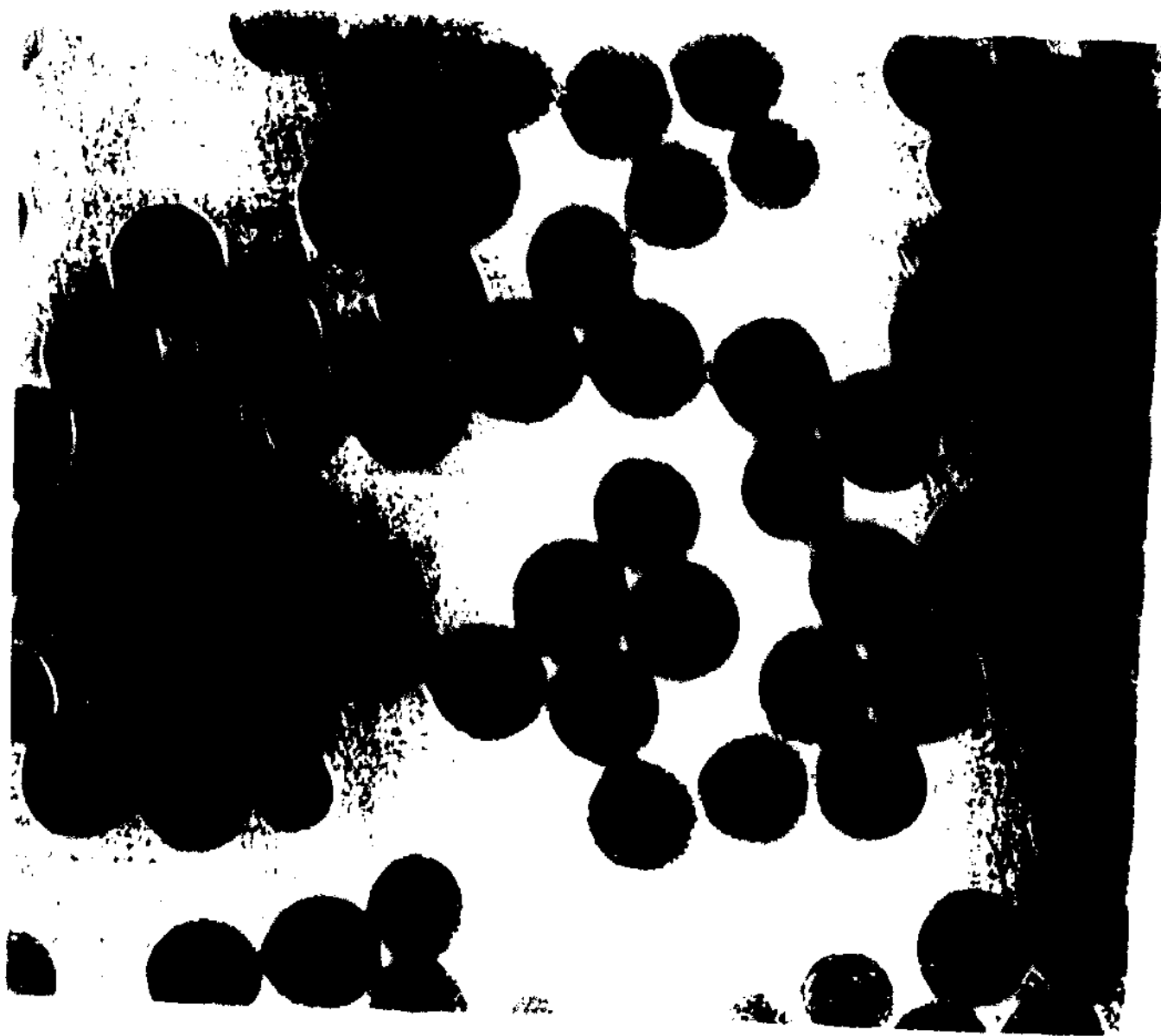
Another discovery made was that to resuspend a flocculated suspension by manually breaking up the flocculate was not the best method. During pressurization, a film of flocculate would form around the dialysis sack for the larger suspensions. Breaking the film only causes the formation of a large mass of flocculate in the sack with only a little liquid to dissolve it. Instead, it was better to hold the double-knotted end of the dialysis sack with one hand and the clipped end in the other and shake the contents of the sack horizontally until the film coating is gone or very thin. This

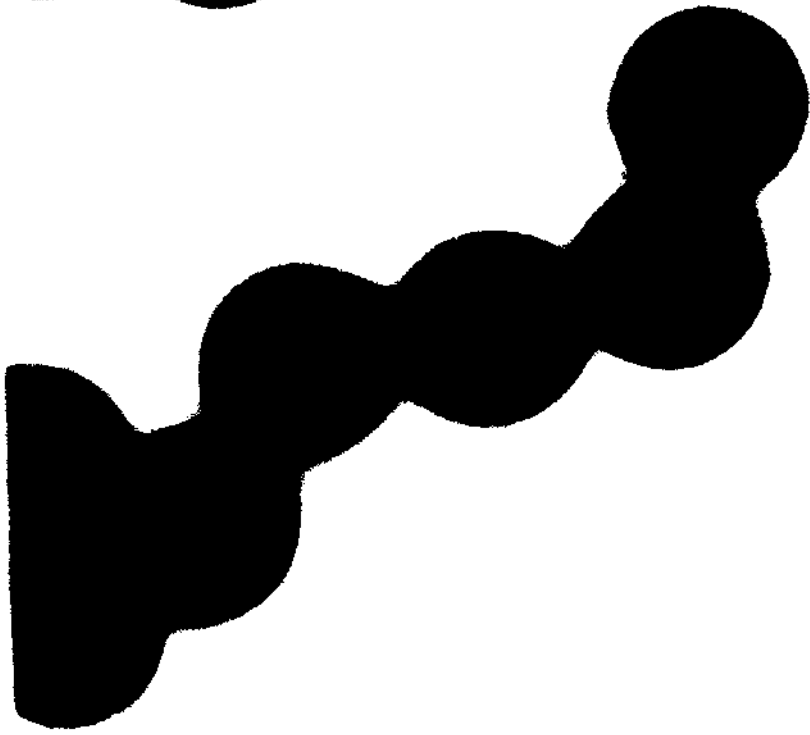
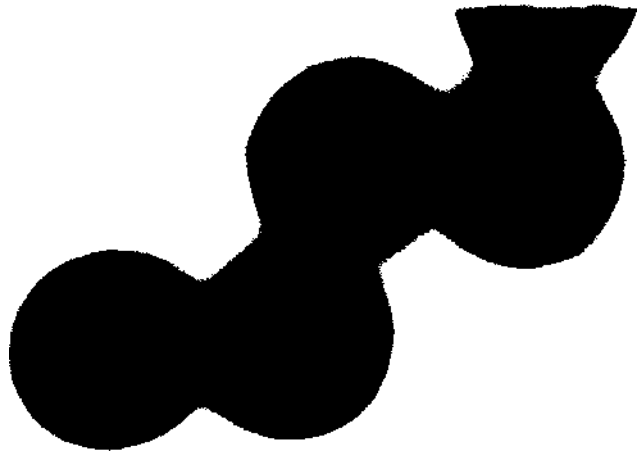
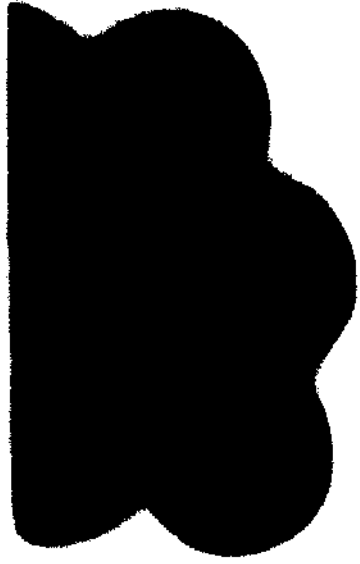
helped prevent the formation of small clumps of flocculate that could not be felt while trying to manually break the flocculates. Trying to redisperse a flocculated suspension by using an ultrasonic cleaner did not work.

A 1:1 by volume fraction sample of flocculated polystyrene was placed in an ultrasonic cleaner to be resuspended. After 30 minutes in the ultrasonic cleaner and vigorous mixing, the flocculated material seemed to be resuspended. The suspension was removed from the cleaner. Ten minutes after removal, the suspension became the consistency of whip cream and gave erroneous results in the shearometer (a negative shear modulus). When the suspension was placed back into the ultrasonic cleaner, the suspension became fluid after 10 minutes. Removal again caused the suspension to have the consistency of whip cream. The flocculation problems did not occur with the 103.9nm particles and shear data was obtained.

After these problems with the particles in a high ionic strength medium, the ionic strength used was cut ten-fold. Three different sized particles were synthesized. These particles made were cleaned by dialysis. When the particles were cleaned, TEM photographs were taken. The particles were homogeneous and were 103.9nm (Fig 4-1a) 386nm (Fig 4-1b), and 523.4 nm (Fig 4-1c) in diameter respectively. The 386nm particles and the 523.4nm particles showed iridescence when concentrated, the 103.9nm particles looked purplish.

The concentrated lattices were sheared to give the results shown in Tables 2 and 3. There were several attempts to increase the volume fractions of the 523.4nm and 386nm particles to get higher shear modulus, but irreversible flocculation occurred. Eventually all of the 523.4nm particles had flocculated and no more shear data could be taken for that system. The volume fraction that this occurred was 0.667. A sample of 382nm particles were also irreversibly flocculated, at a volume fraction of 0.6164. The volume fraction at which these particles flocculated is very close to the ϕ_m of rep packing. This may support the presence of rep packing versus fcc packing for larger particles, because volume fractions around .74 may not even be possible. These values also give an idea as to how high a volume fraction may be attempted to obtain shear modulus for future experiments. The particles that had been leftover from my experiments were given to a graduate student in Zukoski's group.





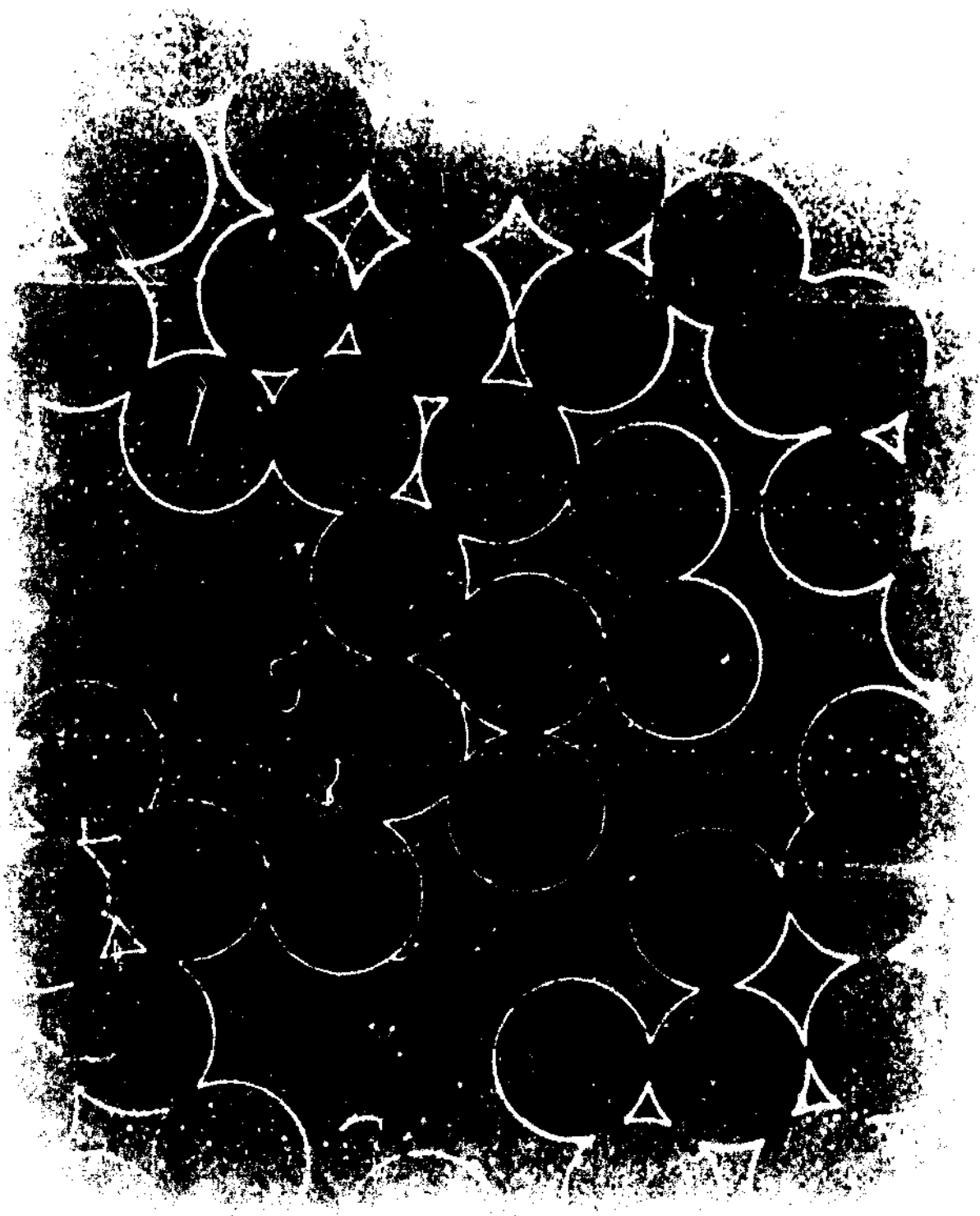


Table 3

Shear Measurements

300nm particles (in 1×10^{-4} NaCl):

<u>Volume Fraction (volume solid/volume solution)</u>	<u>Shear (kPascals)</u>
.4778	.179600
.4778	.180620
.4950	.417599
.5747	2.31905

523.4nm particles (in 1×10^{-4} NaCl)

<u>Volume Fraction (volume solid/volume solution)</u>	<u>Shear (kPascals)</u>
.5035	.55200
.5035	.56100
.5120	.70633
.5182	.83000
.5320	.90369
.5320	.91090
.5320	.91090
.53350	1.21565
.53350	1.18682
.54980	1.94200
.55520	.97166

Table 2

Shear Measurements

103.9nm particles (in 1×10^{-3} NaCl):

<u>Volume Fraction [volume solid/volume solution]</u>	<u>Shear [kPascals]</u>
.3187	.68021
.3240	.52884
.3240	.53697
.3307	.68018
.3307	.68525
.3500	.85940
.3626	1.36068
.3670	1.29547
.3670	1.30265
.3750	1.55447

103.9nm particles (in 1×10^{-4} NaCl)

<u>Volume Fraction [volume solid/volume solution]</u>	<u>Shear [kPascals]</u>
.2735	.583650
.2735	.587710
.2911	.649229
.2966	.748880
.2966	.753960
.2993	.797920
.2993	.804020
.4070	1.34647

4.2 Results of Modeling Studies

A plot of shear modulus vs. volume fractions for the suspensions is shown in Figure 4-2a. The plots had been fitted with an exponential curve in order to more clearly illustrate the data obtained. As can be seen by Fig 4-2a, the measured points form a smooth exponential curve as would be predicted by the Buscall (eqn 8) and the Russel (eqn 9) equations. However, when the RLSAP, RLSACP, RLSALCP, and the RLSAPDHS modeling programs for shear modulus were applied, there were discrepancies between the program and the measured data. Tables 4 and 5 give values of surface potential for each curve.

For the 103.9nm particles in either 10^{-4}M or 10^{-3}M NaCl solution (Figures 4-2bi to 4-2ci), the assumption that the particles were in an FCC configuration seemed to be the most accurate assumption. The best model for the data obtained was the RLSAP. Overall, the worst modeling program was RLSACP.

The modeling programs for the 523.4nm particles and the 386nm particles did not work very well. All of programs failed to catch the steepness of the modulus curves measured. As can be seen by Figure 2a, the curves for 523.4 and 386nm particles are more steeper than for either 103.9nm measurements. The reason for this is unclear, the ionic strength within the suspension may be more heavily dependent on volume fraction than suggested by Penfold and Ramsey or Voeglti. The intersection of the modeling curves with measured data around a volume fraction of 0.53 may suggest this since previous research in shear modulus behavior was only up to 200nm in size and less the 0.40 in volume fraction. For the modeling programs, it seems that the RCP assumption works better than FCC because these curves are slightly more steeper.

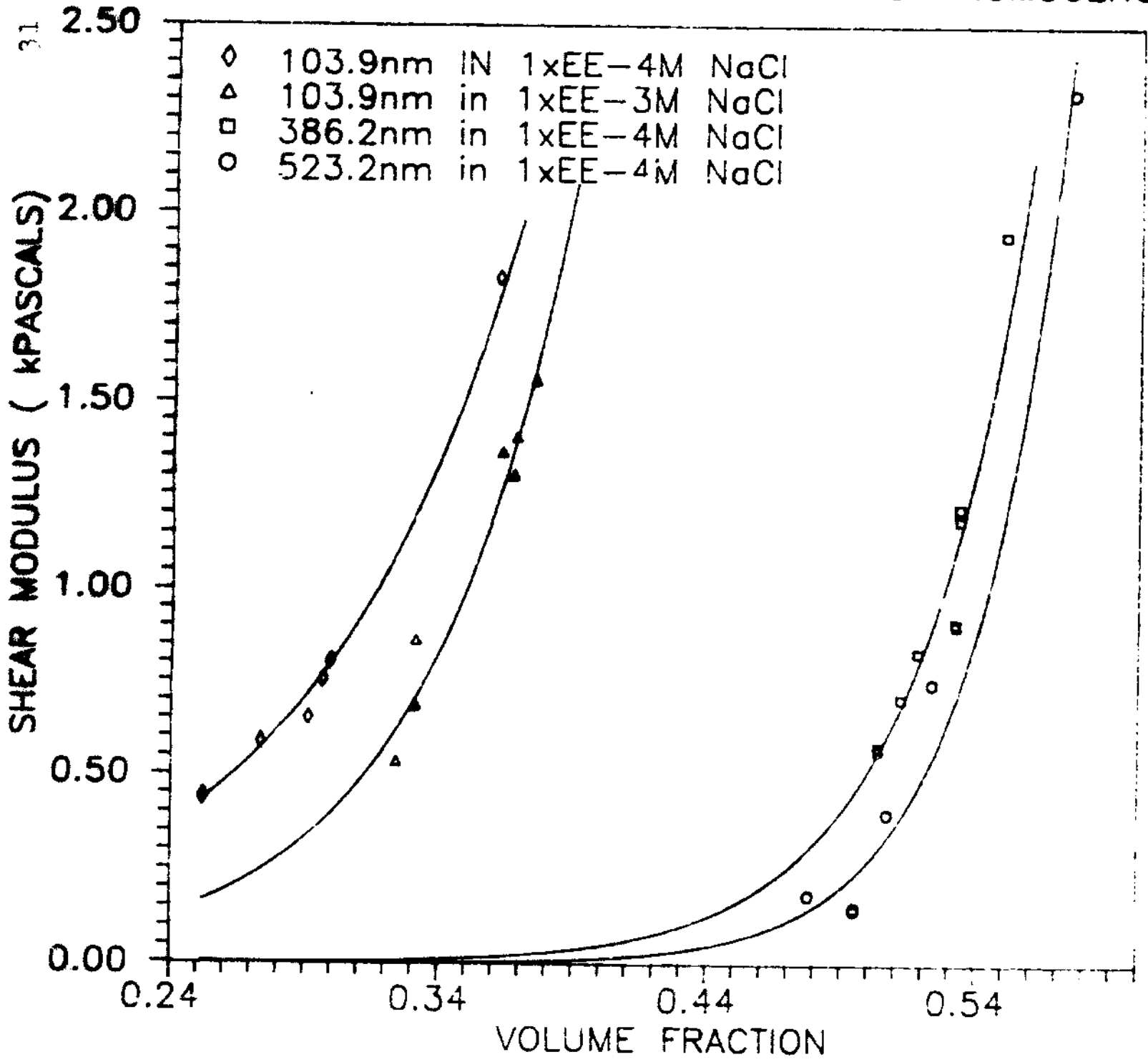
Table 4: Surface Potential of Shear Modulus Program Models

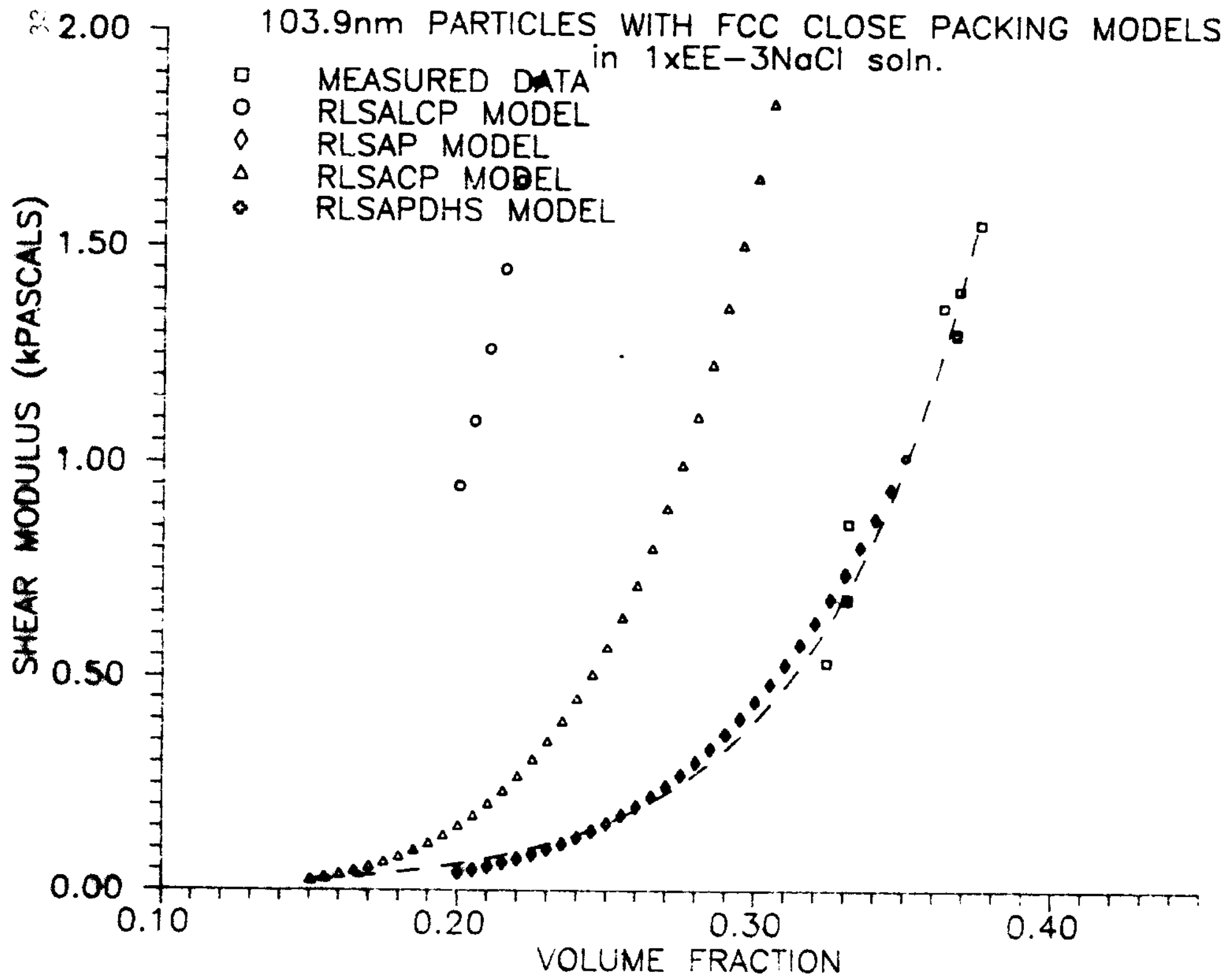
Model	[NaCl]	Particle Diam. (nm)	ϕ	ψ_0	
RLSAP	10 ⁻⁴ M	523.4	.74	21.59mV	
	10 ⁻⁴	386	.74	16.93	
	10 ⁻⁴	103.9	.74	11.90	
	10 ⁻³	103.9	.74	12.21	
	10 ⁻⁴	423.4	.64	13.95	
	10 ⁻⁴	386	.64	11.92	
	10 ⁻⁴	103.9	.64	10.87	
	10 ⁻³	103.9	.64	12.21	
	RLSALCP	10 ⁻⁴	523.4	.74	21.67
		10 ⁻⁴	386	.74	15.26
		10 ⁻⁴	103.9	.74	11.34
		10 ⁻³	103.9	.74	64.35
10 ⁻⁴		523.4	.64	13.43	
10 ⁻⁴		386	.64	11.10	
10 ⁻⁴		103.9	.64	10.34	
10 ⁻³		103.9	.64	68.13	

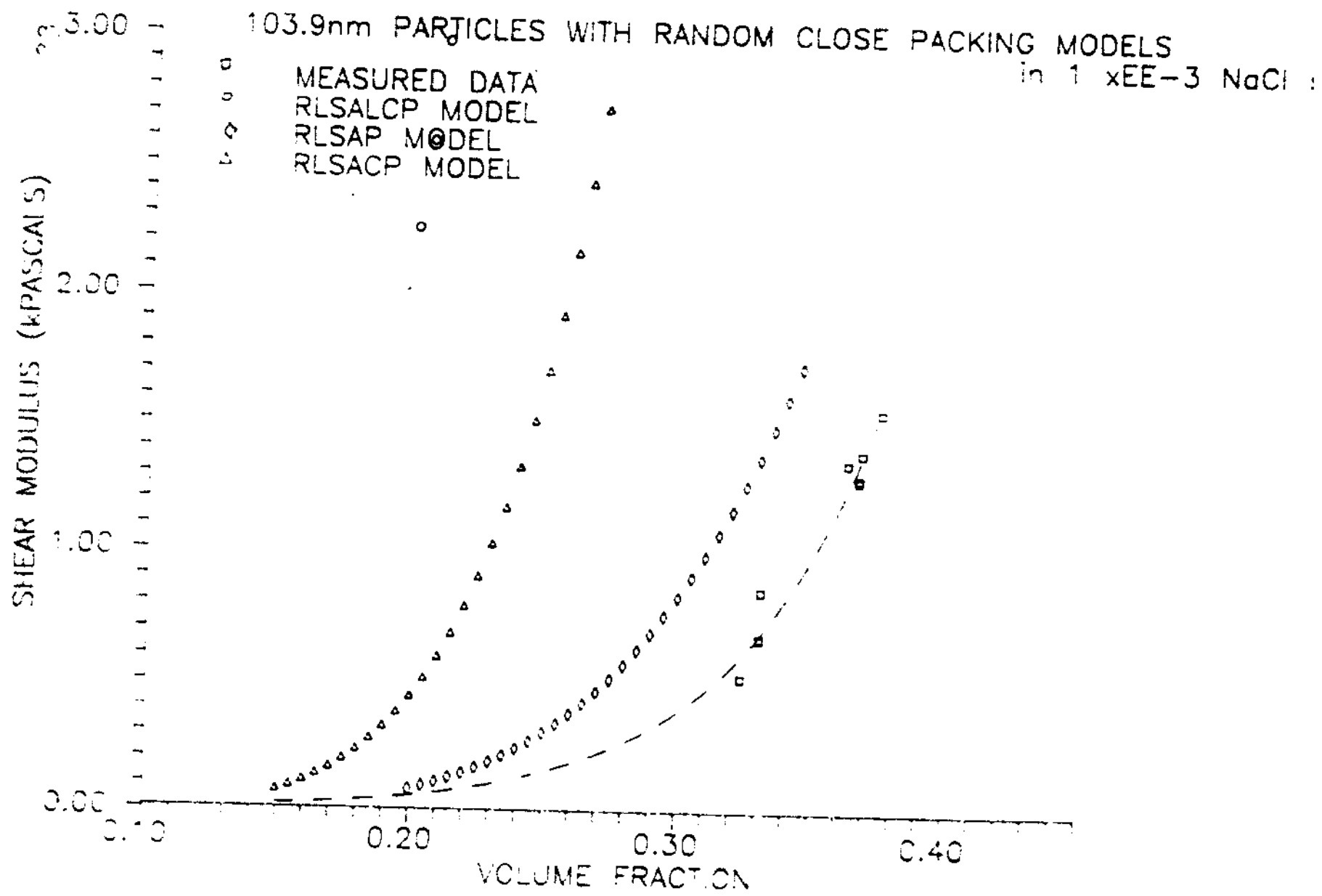
Table 5: Surface Potentials for RLSACP and RLPDHS

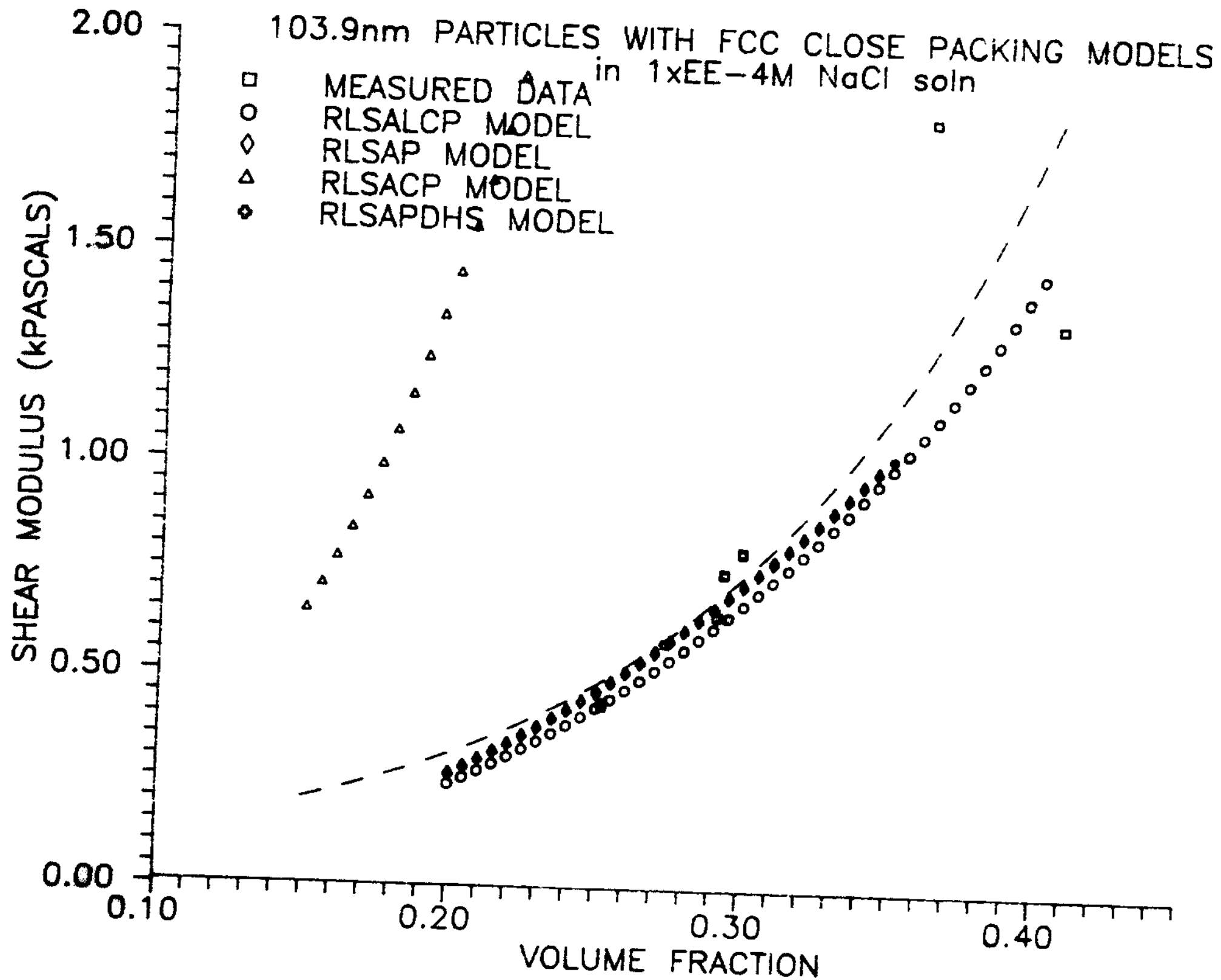
Model	[NaCl]	Particle Diam. (nm)	ϕ	Ψ_Q
RLSACP	10 ⁻⁴	523	.74	62.44mV
	10 ⁻⁴	386	.74	67.55
	10 ⁻⁴	103.9	.74	51.91
	10 ⁻³	103.9	.74	51.10
	10 ⁻⁴	523	.64	13.06
	10 ⁻⁴	386	.64	10.26
	10 ⁻⁴	103.9	.64	70.66
	10 ⁻³	103.9	.64	66.78
RLPDHS	10 ⁻⁴	523.4	.74	11.08
	10 ⁻⁴	382.6	.74	10.16
	10 ⁻⁴	103.9	.74	11.98
	10 ⁻³	103.9	.74	14.23

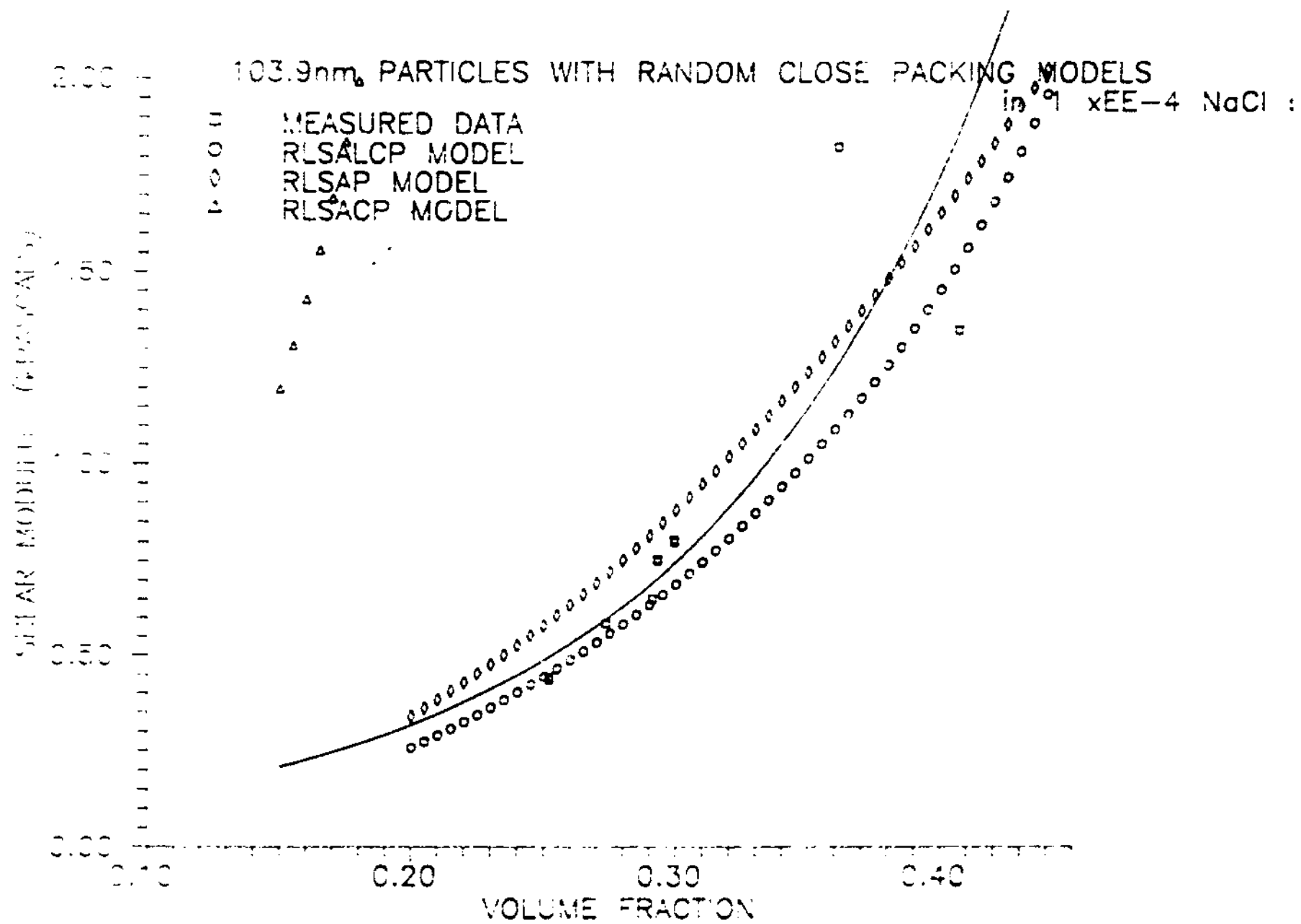
SHEAR MODULUS vs. VOLUME FRACTION FOR HOMOGENOUS PARTICLES



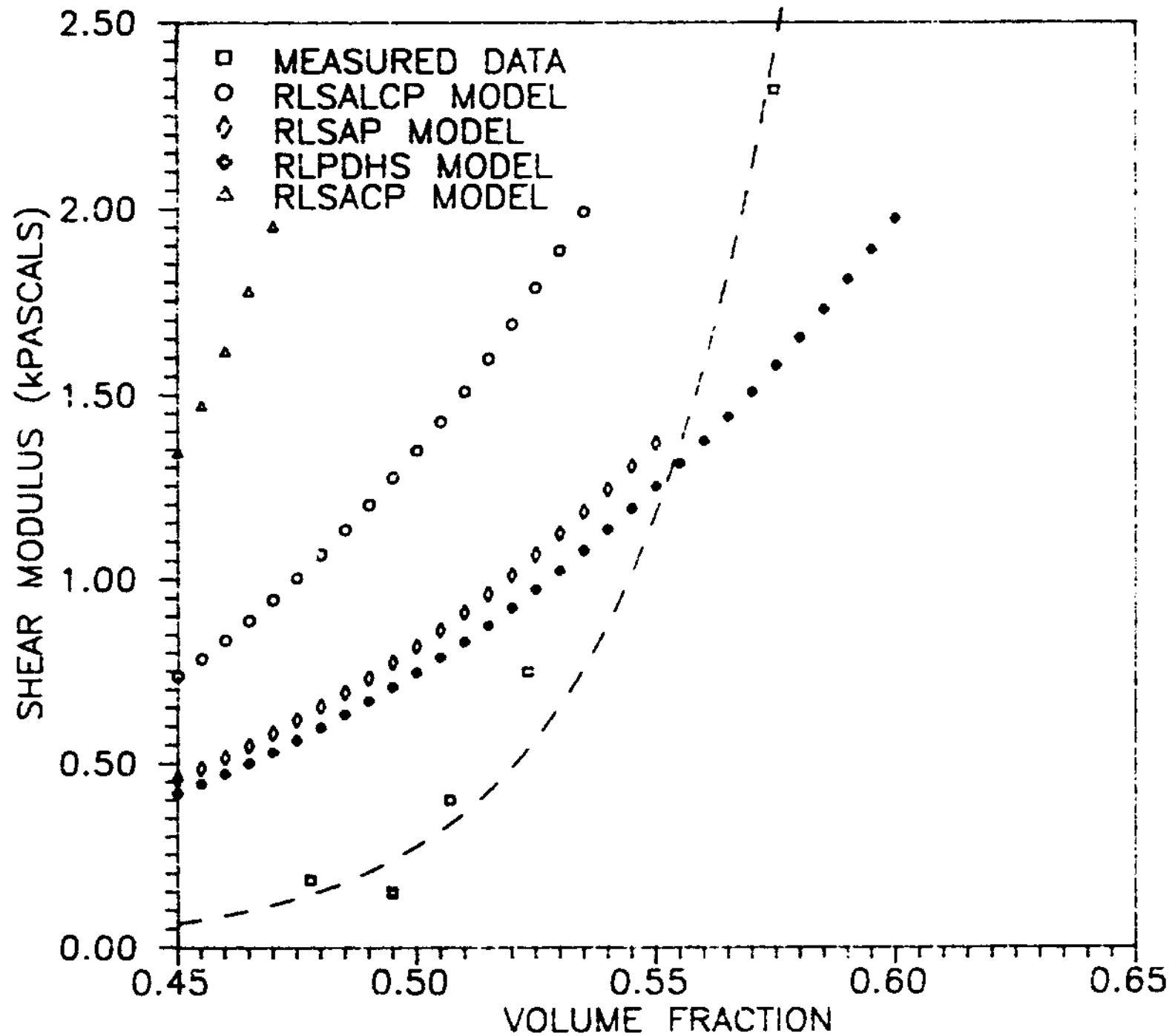




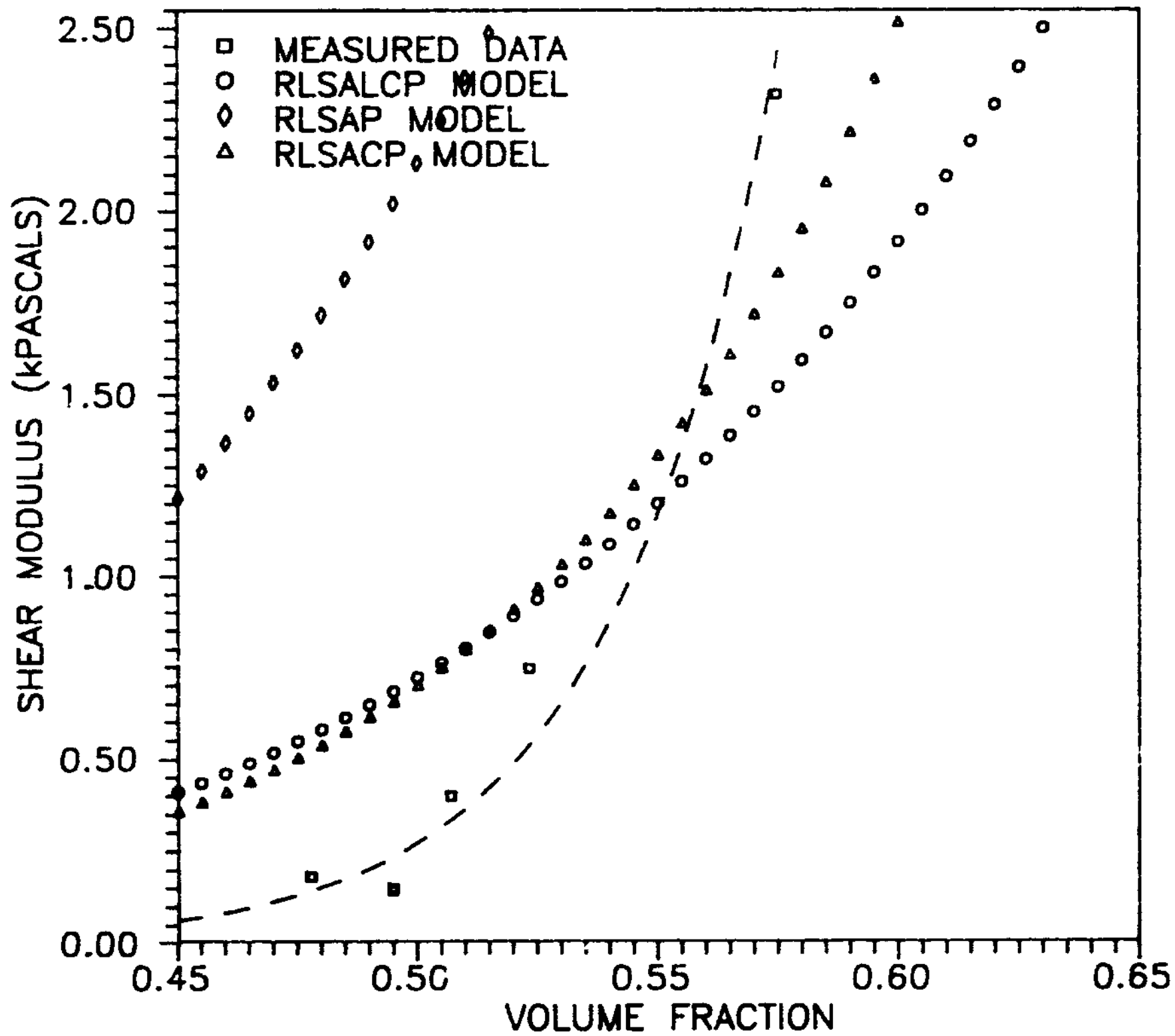




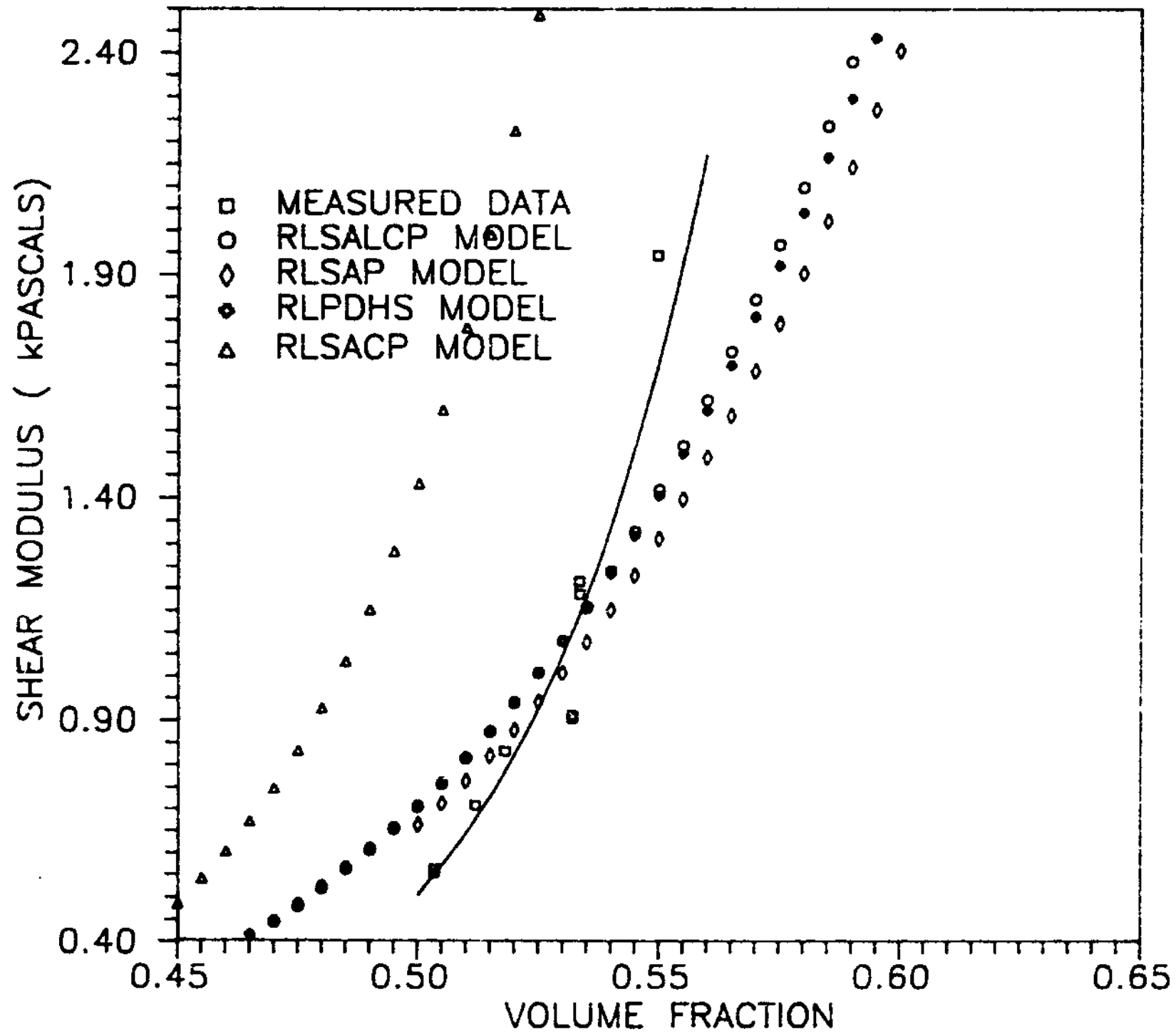
386nm POLYSTYRENE PARTICLES IN 1.5×10^{-4} NaCl
WITH FCC PACKING CURVE MODELS



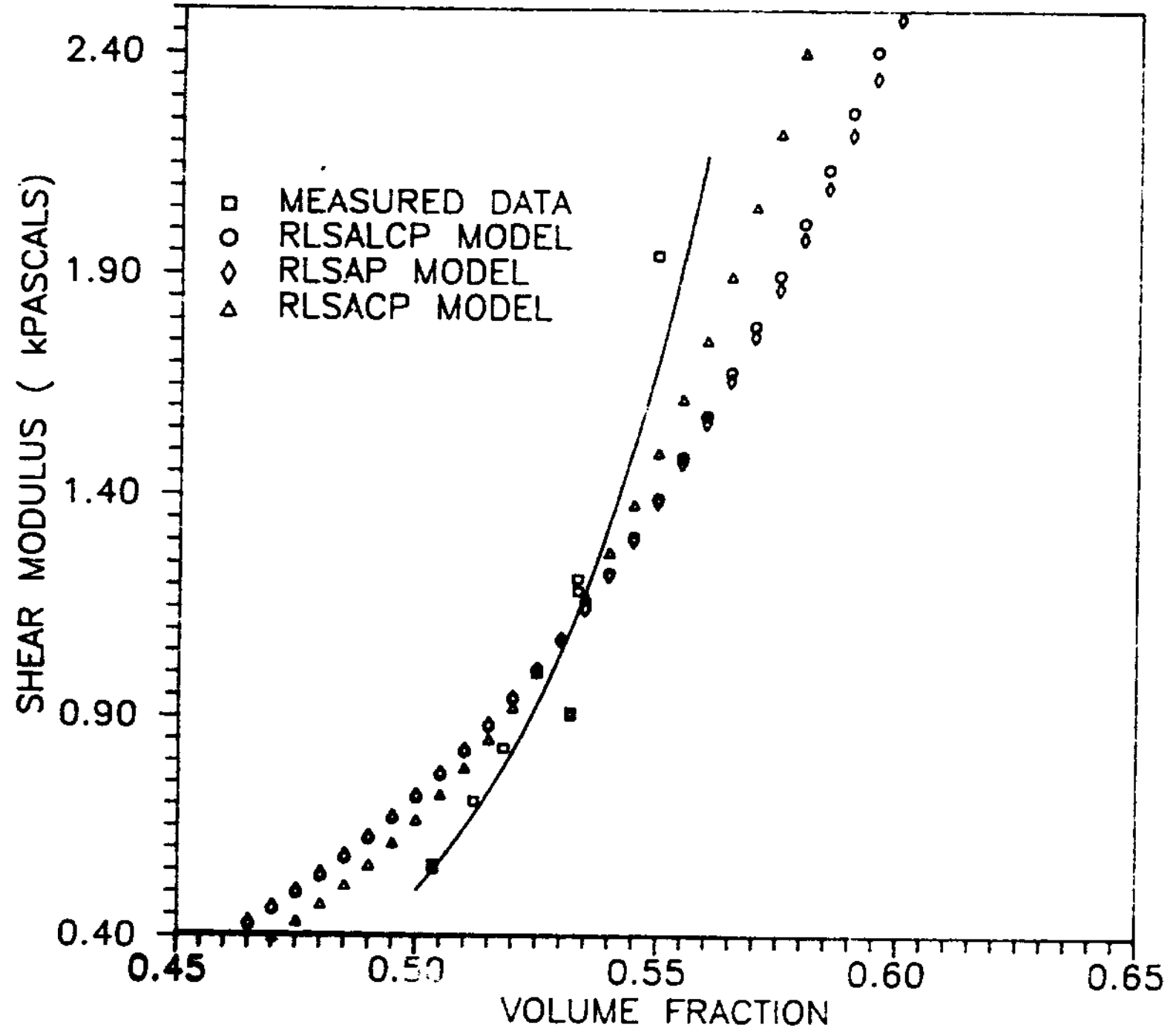
386nm POLYSTYRENE PARTICLES IN 1×10^{-4} NaCl
WITH RANDOM CLOSE PACKING CURVE MODELS



523.4nm PARTICLES WITH FCC PACKING MODELS



523.4nm PARTICLES WITH RANDOM CLOSE PACKING CURVE MODELS



5.0 Conclusion

- 1) The modeling programs used in this research may not be able to accurately predict the shear modulus behavior of particles larger than 200nm.
- 2) There is a definite divergence of measured shear modulus data and predicted shear modulus behavior. These two curves intersect at the same point for both the 523nm and 386nm particles, around a volume fraction of 0.53.
- 3) Further research in the shear behavior of large particles at high volume fractions is limited to a volume fraction of roughly 0.63
- 4) The volume fraction limit of 0.63 may suggest that FCC packing is not possible for larger particles.
- 5) The assumption for FCC packing seems to be better in modeling the shear modulus behavior of 103.9nm particles. The best modeling program seems to be RLSACP.
- 6) The assumption for RCP packing seems to be better in modeling shear modulus behavior for 386nm and 523nm particles. The best modeling program seems to be RLSACP.
- 7) The shallowness of the modeling curves to measured data suggests that the ionic strength of the suspension is more heavily dependent on volume fraction than is predicted by Penfold and Ramsay or Voegli.

6.0 Recommendation

1) During the concentration of the suspension, if a film of flocculated material occurs around the dialysis sack do not try to break it up and resuspend it. Breaking the film only causes the formation of a large mass of flocculate in the sack with only a little liquid to dissolve it. Instead, hold the double-knotted end of the dialysis sack with one hand and the clipped end in the other and shake the contents of the sack horizontally until the film coating is gone or very thin. This may also help in the presence of small clumps of flocculate that cannot be felt while trying to manually break the flocculates.

2) Design a open rack for pressurizing particles. The problem with current pressurizing sacks is that when a dialysis sack begins to leak, the rack had to be pulled out of the container; the sack removed, fixed, and replaced. This process of taking the rack out, or even just fumbling with the sacks in the rack would usually cause another sack to leak. This can be infuriating at times. Instead use a weighted rack that has a lid on top to hold the nitrogen tubes and place this assembly in a 25l garbage pail. That way, leaking sacks can be removed more easily without harming the sacks. In addition, this design would make it a lot easier to check for flocculates in the dialysis sack and allow the researcher to check on sack more often.

3) Another quick method to check if newly synthesized particles are monodispersed is by placing the emulsion on a glass slide and allowing it to dry. This method allows the floors and tables to be clean and also one can manipulate the slide in the light to see if the particles show iridescence.

4) Further research should be done as to whether the 60% volume fraction limit applies in general. Whenever flocculation occurs, a sample should be saved for a volume fraction to be taken.

Bibliography

- [1] Buscall, Richard and Goodwin, James W. " Viscoelastic Properties of Concentrated Latices." J. Chem. Soc., Faraday Trans. 1 Vol 78 pp2889-2899 (1982)
- [2] Derjaguin, B. and Landau, L. Acta Physiochem. URSS Vol 14, p663 (1941)
- [3] Verwey, E.J.W. and Overbeek J.Th.G. Theory of the Stability of Lyophobic Colloids. Elsevier Press. Amsterdam (1948)
- [4] Levine, S. Disc. of Faraday Soc., Vol 18 p202 (1954)
- [5] Hamaker, H.C. Physica. Vol 4 p1058 (1937)
- [6] Tadros, Th. F., Colloids and Surfaces. Vol 18 p137 (1986)
- [7] Bossis, G. and Brady J.F. Journal Chemical Physics. Vol 87(9) p.5437 (1987)
- [8] DeKruif, C.G., Van Fersel E.M.F. and A. Vrig. Journal of Chemical Physics. Vol 83(9) p4717 (1985)
- [9] Russel, W.B. Journal Chemical Physics. Vol 84(3) p1815 (1986)
- [10] Penfold, Jeff and Ramsay, John D.F., Journal of Chemical Society, Faraday Trans. 1 Vol 81 p117 (1985)
- [11] Voegli, Leo. Electrostatic and Electrokinetic Properties of Concentrated Suspensions of Polystyrene Lattices. MS Thesis, University of Illinois at UC (1988)
- [12] Lindsay, H.M. and Chaiken, P.M. Journal Chemical Physics. Vol 76(7) p3774 (1982)

- [13] Lindsay, H.M. and Chaiken, P.M. J. de Physique Vol 46(3), C3-269, (1985)
- [14] Lindsay, H.M., Dozier, W.D., Chaiken, P.M., Klein and Walker Hess, Journal of Phys. A Vol 19, p2585 (1986)
- [15] Juang, Mike and Krieger, Irvin M. "Emulsifier-Free Emulsion Polymerization with Ionic Comonomer" Journal of Polymer Science, Vol 14 pp2089-2107 (1976)
- [16] Liu, Li Jen and Krieger, Irvin M. "Emulsifier-Free Polymerization with Ionic Comonomer" Journal of Polymer Science, Vol 19 pp3013-3026 (1981)
- [17] Rank Pulse Shearometer Instruction Manual. (1986 ed.)
- [18] van Olphen, H. Clays Clay Miner. Vol 4 p204 (1956)
- [19] Goodwin, J.W. and Khidher, A.M. Colloid and Interface Science, ed. M. Kerker Academic Press, New York (1976)
- [20] Buscall, Richard; Goodwin, James W.; Hawkins, Michael W. and Ottewill, Ronald H. "Viscoelastic Properties of Concentrated Latices-Part I- Methods of Examination" J Chem Soc., Faraday Trans. I Vol 78 pp2873-2887 (1982)
- [21] Jeanne Chang

Appendix A1: Theory of Shearometer

The instrument used in measuring the shear modulus of the polystyrene lattice was a Rank Pulse Shearometer by Pen Kem Inc.[17]

A1.1 History and Theory

The shearometer was developed by van Olphen [18] for the study of montmorillonite gels and further developed by Goodwin and Khidher [19]. The pulse shearometer was designed to measure the storage modulus of a suspension at moderate frequencies. The primary unit of this device is the shear-wave propagation cell.

The shear-wave propagation cell consists of 3 parts, the upper transducer, the lower transducer and the glass barrel (Fig A1)[17]. The upper and lower transducers have a similar design. A piezoelectric crystal is connected by a shaft to a 2.5cm in diameter stainless steel disk in order to receive or generate a torsional shear wave in the medium. A pulse generator supplies a transient electrical pulse of 200 Hz to the lower transducer which causes the lower disk to rotate about 10^{-4} radians. This generates the torsional shear wave within the medium. When the pulse is generated to the lower transducer, the upper transducer is monitored by an oscilloscope. The pulsed wave travels through the medium to the disk on the upper transducer. The upper disk responds to the propagated shear wave by rotating. The rotation of the upper disk causes a strain to be applied to the piezoelectric crystal, generating a current. The current generated in the upper transducer is measured by the oscilloscope and calibrated by a 10^3 Hz square wave. The oscilloscope pattern received by the upper transducer consists of a linear portion followed by a damped sine wave. The arrival of the sine wave corresponds to the arrival of the propagated shear wave to the upper transducer. Since the oscilloscope trace was started when the pulse was initially generated at the lower transducer, the length of time before the first peak of the sine wave is measured and converted to a propagation time, Δt , by calibration to the square wave. The slope from a plot of disk separation vs. propagation time was measured to give the shear wave velocity. The shear modulus can be found by using the following equation:

$$G = \rho v^2 \quad (A1)$$

where G = shear modulus (Pa)

ρ = density (kg/m^3)

v = shear wave velocity (m/s)

A1.2 Derivation of Shear Modulus Equation (A1)

Equation (A1) allows the shear modulus of a suspension to be determined by only two parameters, density and shear wave velocity. The derivation of this simplified calculation for the determination of shear modulus by torsional straining is presented.

When a viscoelastic fluid is exposed to an oscillatory shearing strain, the shear modulus of the fluid can be described by a frequency domain equation consisting of two parts, the storage modulus and dissipative modulus.

$$G^*(\omega) = G'(\omega) - i \omega \eta'(\omega) \quad (A2)$$

where $G^*(\omega)$ is the shear modulus

$G'(\omega)$ is dynamic rigidity; function of ω

$\eta'(\omega)$ is dynamic viscosity; function of ω

ω is angular frequency of deformation

Under steady state flow conditions ($\omega = 0$) G' vanishes and purely viscous behavior is observed. The viscosity under these conditions is defined as :

$$\eta(0) = \lim_{\omega \rightarrow 0} \eta' \quad (A3)$$

In unsteady state conditions, $\omega > 0$, both the storage modulus and the dissipation modulus are non-zero. However, at very high frequencies, the storage modulus approaches a limiting value where:

$$G_0 = \lim_{\omega \rightarrow \infty} G' \quad (A4)$$

Therefore by applying a high frequency torsional shear, the storage shear modulus

will equal the shear modulus of the suspension. The storage shear modulus is a function of the wave velocity, u , and the density of the sample:

$$G' = u^2 \rho \frac{(1 - r^2)}{(1 + r^2)^2} \quad (\text{A5})$$

where: $r = 2\lambda / 2x_0$

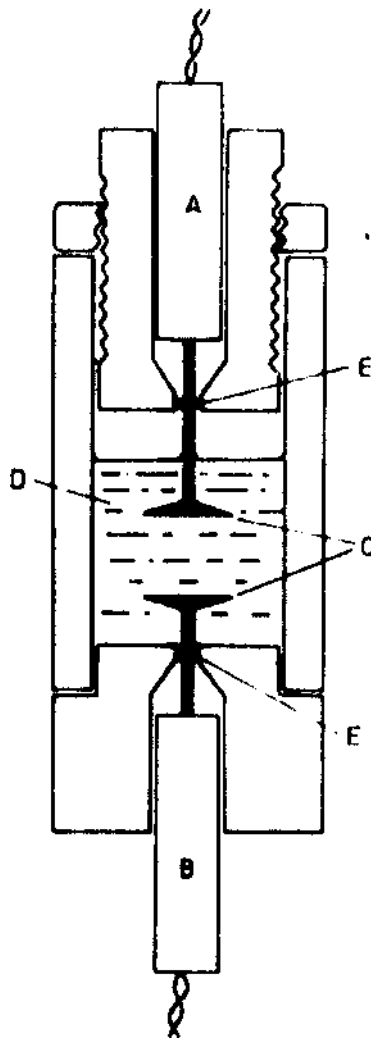
$\lambda = 2\pi u / \omega$ length of wavelength [m]

$x_0 =$ critical damping length [m]

In order to completely define G' , u and r need to be known. However since the term r is small enough to become negligible, equation (A5) simplifies to [20]

$$G = \rho v^2 \quad (\text{A1})$$

R. BUSCALL, J. W. GOODWIN, M. W. HAWKINS AND R. H. GIFFWILL 2875



Nomenclature

A	Hamaker constant
a	particle radius (m)
e	charge of electron (C)
G_{ACT}	Actual shear of suspension (Pa)
G₁₀₀₀	Shear when density initially assumed to be 1000kg/m ³
G₀	Shear Modulus (Pa)
I	Ionic Concentration (mol/liter)
k	Boltzman constant (J/K)
n	# of nearest neighbors
N	Avogadro's number (mole ⁻¹)
R	Distance from center to center between particles (m)
T	Temperature (K)
U	Wave velocity (m/s)
V_A	Van der Waals Potential (V)
V_R	Electrostatic Potential (V)
V_T	Total Potential (V)
α	$(3/32) F_m n$
ε	relative permittivity
ε₀	permittivity of free space (F/m)
σ	surface charge (C/m ²)
π	pi
κ	Debye-Huckel Parameter (inverse double-layer) (m ⁻¹)
φ_m	maximum packing fraction
φ	packing fraction
ρ_{ACT}	actual density (kg/m ³)

ρ	number density (# part/ m ³)
ψ_0	diffuse layer potential[surface potential] (V)
y	Phase Potential
λ	$2\rho u/\omega$ length of wavelength (m)
$\eta'(\omega)$	dynamic viscosity (Pa-s)
$G^*(\omega)$	shear modulus (Pa)
$G'(\omega)$	dynamic rigidity (Pa)

Programs

RLSAP	Russel Eqn. with LSA approximation using ψ
RLSACP	Russel with LSA using Penfold & Ramsey and ψ
RLSALCP	Russel, LSA, Leo Voegli model with ψ
RLPDHS	Russel, using Hard Sphere Model, LSA